Study of the Kinetics and Equilibrium of the Benzyl-Radical Association Reaction with Molecular Oxygen

FREDERICK F. FENTER*, BARBARA NOZIÈRE, FRANÇOISE CARALP, and ROBERT LESCLAUX

Laboratoire de Photophysique et Photochimie Moléculaire, Université de Bordeaux I, 351 Cours de la Libération 33405 Talence Cedex, France

Abstract

The forward rate constant, k_1, and the equilibrium constant, K_p, for the association reaction of the benzyl radical with oxygen have been determined. The rate constant k_1 was measured as a function of temperature (between 298 and 398 K) and pressure (at 20 and 760 torr of N_2) by two different techniques, argon-lamp flash photolysis and excimer-laser flash photolysis, both of which employed UV absorption spectroscopy (at 253 nm and 305 nm, respectively) to monitor the benzyl radical concentration. Over the range of conditions studied, we find that the reaction is independent of pressure and is almost independent of temperature, which is in accord with two early studies of the reaction but in apparent disagreement with more recent work. For our results in 760 torr of N_2 and for $298 < T/K < 398$, a linear least-squares fitting of the data yield the expression: $k_1 = (7.6 \pm 2.4) \times 10^{-13} \exp[(190 \pm 160)\mathbf{K/T}]$ cm^3 molecule^{-1} s^{-1}. With the flash-photolysis technique, we determined K_p over the temperature range 398–525 K. Experimental values were analyzed alone and combined with theoretically determined entropy values of the benzyl and benzylperoxy radicals to determine the enthalpy of reaction: $\Delta H^\circ_{298} = (-91.4 \pm 4)$ kJ mol^{-1}. Previous work on the benzyl radical enthalpy of formation allows us to calculate ΔH°_{f298} (Benzylperoxy) = (117 ± 6) kJ mol^{-1}. In addition, we carried out an RRKM calculation of k_1 using as constraints the thermodynamic information gained by the study of K_p. We find that all the studies of the association reaction are in good agreement once a fall-off effect is taken into account for the most recent work conducted at pressures near 1 torr of helium.

Introduction

An elementary process in the oxidation of alkyl radicals, both in flames and in the atmosphere, is the association reaction of these species with molecular oxygen [1,2]. Because of their practical importance, the kinetics and equilibria for a growing number of these alkyl-radical reactions have been studied over appropriately broad ranges of pressure and temperature:

$$R + O_2 \underset{}{\overset{[M]}{\longrightarrow}} RO_2$$

Recent work from this lab, carried out collaboratively with Gutman and co-workers, [3–5] has demonstrated the utility of studying this type of reaction by three complementary efforts, including (1) an experimental determination of the rate constant for association as a function of temperature and pressure, (2) an experimental measurement of the equilibrium constant, yielding the thermodynamic parameters

*Current Address: Laboratoire de Pollution Atmosphérique et Sol, Département de Génie Rural, Ecole Polytechnique Fédérale de Lausanne, CH-1015 Lausanne, Switzerland.

International Journal of Chemical Kinetics, Vol. 26, 171–189 (1994)
 CCC 0538-8066/94/010171-19

for the chemical reaction, and (3) a RRKM theoretical calculation. The goal of the last is to use the thermodynamic parameters derived from the equilibrium constants as constraints on a global fitting of the $k(M,T)$ for the association reaction, which both establishes a pleasing cohesion of the experimental elements and provides a framework from which rate constants can be derived for specific conditions of pressure and temperature.

The benzyl radical is of some interest in atmospheric chemistry and combustion because it is a product of the oxidation of toluene, which is widely used as a fuel additive [6]. For this reason, the oxidation pathways of toluene, and therefore of the benzyl radical, has been the subject of a number of previous studies [7–10]. Based on the results of two early studies, the rate constant for the association reaction of the benzyl radical with oxygen, k_1, was thought to be independent of both pressure and temperature:

(1)
$$C_6H_5CH_2 + O_2 \xrightarrow{[M]} C_6H_5CH_2O_2$$

Ebata et al. reported the value $k_1 = 0.99 \times 10^{-12}$ cm^3 molecule^{-1} s^{-1}; they observed no pressure dependence between 160 mtorr of benzyl bromide and 160 torr of nitrogen [7]. Nelson and McDonald [8] later measured k_1 in nitrogen and found no variation as a function of temperature (298 and 373 K) or pressure (3 and 15 torr or N_2), and their reported value of 1.05×10^{-12} cm^3 molecule^{-1} s^{-1} is in excellent agreement with Ebata et al. More recently, Bartels et al. [9] determined an upper limit of 5×10^{-13} cm^3 molecule^{-1} s^{-1} for k_1. In addition, Devolder and co-workers [10] have reported a series of experiments conducted at pressures near one torr of helium using the discharge-flow technique; in addition to finding the somewhat lower value of $k_1(298)$ of 7.2×10^{-13} cm^3 molecule^{-1} s^{-1}, they reported a marked temperature dependence at the same pressure, with the k_1 dropping to the value of 2.0×10^{-13} cm^3 molecule^{-1} s^{-1} at the highest temperature studied, 433 K, although these high temperature values were derived indirectly from experiments designed to determine the equilibrium constant for the reaction [10]. The results of the previous kinetic studies of reaction (1) are summarized in Table I.

The study by Elmaimouni et al. represents the only previous determination of the equilibrium constant for reaction (1) [10]. In that work, the equilibrium between benzyl and peroxybenzyl radicals was followed as a function of temperature and

TABLE I. Summary of previous determinations of k_1.

T (K)	P (torr)	Bath gas	$k_1/10^{12}$ [a]	Method[b]	Reference
298	0.2–160	N_2 [c]	0.99 ± .05	LP/LIF	[7]
295–372	3–15	N_2	1.05 ± .1	LP/LIF	[8]
293	0.75–3.0	He	>0.5	DF/MS	[9]
298	1.0	He	0.72	DF/LIF	[10]
353	1.0	He	0.45	DF/LIF	[10]
433	1.0	He	0.3 ± .10	DF/LIF	[10]

[a] Units for k are cm^3 molecule^{-1} s^{-1}.

[b] LP: Laser flash photolysis; DF: discharge flow; LIF: Laser-induced fluorescence; and MS: mass spectrometry.

[c] The low-pressure experiments were conducted with 160 *m*torr of benzyl bromide as the bath gas.

oxygen concentration in a discharge-flow reactor in one torr of helium. Applying both Second-Law and Third-Law analyses, they were able to derive the value of $\Delta H^{\circ}_{298} = (-84 \pm 5)$ *k*joule mol^{-1} for the reaction. This value seems to confirm the suggestion that the $R - O_2$ bond energy for radicals with resonantly stabilized *R*-groups is expected to be significantly smaller than for other alkylperoxy radicals.

We undertook the present study of the kinetics and equilibrium of reaction (1) in an attempt to resolve some of the interesting issues raised by the study of Elmaimouni et al. In particular, the temperature dependence of the forward rate constant that they report seems at odds with the previous work on k_1. Our study consists of three distinct efforts: (1) the study of the forward rate constant, k_1, by two experimental techniques over a significant range of pressure and temperature; (2) the study of the equilibrium constant at ambient pressure over a temperature range that is significantly larger (398–525 K) than in the study by Elmaomouni et al. (393–433 K); and (3) a theoretical treatment of the kinetic results, using the derived thermodynamic parameters from the equilibrium determination, that provides a new perspective on the kinetics of reaction (1). Based on this work, we will be able to present a series of parameters from which the rate constants for both the association (k_1) and dissociation (k_{-1}) can be calculated with relative certainty over a significant range of pressure or temperature. We will also be able to draw some conclusions concerning the thermochemistry of the benzylperoxy radical, which is important for the assessment of other possible mechanistic pathways for this radical under conditions relevant for combustion and atmospheric chemistry.

In this study, we present the experimental results on the kinetics and equilibrium of reaction (1) using the flash photolysis/UV absorption technique; addition experiments on the forward rate constant were carried out using the laser-flash photolysis/UV absorption technique. We also present a theoretical RRKM analysis which, using the thermodynamic parameters derived from the equilibrium-constant determination, is able to put the ensemble of our and previous experimental work on the forward rate of reaction, k_1, into a coherent framework.

Experimental Details

The two experimental techniques employed in this study have been described recently in the literature. Each is treated below, separately, in abbreviated detail:

Flash-Photolysis/UV Absorption Study

This apparatus is described to greater extent in previous work [11]. It consists of a cylindrical quartz reaction cell (4 cm by 70 cm) which is mounted in an oven that can be heated to 1000 K. The temperature is monitored by a set of thermocouples and regulated to a precision of ±3 K by varying the current to the oven heating elements. A flash of 300 mJ is generated from an argon flash lamp located inside the oven. The benzyl and benzylperoxy radical concentrations are monitored by UV absorption spectroscopy at the wavelength of 253 nm by passing the slightly focussed beam of a deuterium lamp twice through the cell and focussing this light onto the slit of a monochromator. The light level is measured by a photomultiplier tube, whose signal is digitalized and transferred to a microcomputer for signal averaging and analysis.

Benzyl radicals are formed by the near-UV photolysis of Cl_2 in the presence of toluene:

(2) $$Cl_2 + h\nu\ (\lambda > 300\ \text{nm}) \longrightarrow 2Cl$$

(3) $$Cl + C_6H_5CH_3 \longrightarrow HCl + C_6H_5CH_2$$

Unlike the reaction of OH with toluene, which has a significant fraction of an OH ring addition pathway [12], reaction (3) has been found to react solely by the above H-abstraction route [13]. Because the UV absorption cross-section for benzyl is large at 253 nm (about 1.0×10^{-16} cm^2 $molecule^{-1}$ with the spectral resolution employed in this study) [14] we were able to work with very low initial radical concentrations. For both the kinetic and equilibrium experiments carried out by the flash-photolysis technique, the initial concentration of toluene was $3.4–6.5 \times 10^{15}$ molecule cm^{-3}, the concentration of oxygen was varied from $0.55–11.0 \times 10^{15}$ molecule cm^{-3}. For individual experiments, the $[Cl_2]$ was calculated precisely from its absorption at 330 nm [15]. The total pressure of 760 torr was attained by filling with nitrogen. The gas mixtures were prepared by diluting Cl_2, toluene and oxygen into a large flow of nitrogen using calibrated flow controllers. Under these experimental conditions, initial radical concentrations were between $4.5–12.5 \times 10^{12}$ molecule cm^{-3}. The total flow is sufficiently elevated to ensure that the reaction mixture in the cell is completely replenished between each flash. The materials were supplied as follows: Cl_2 (AGA Gaz spéciaux, 5% in N_2, purity >99.9%); O_2 and N_2 (AGA Gaz spéciaux, purity >99.995%); and toluene (Aldrich, purity = 99.98%), which was degassed before use.

Kinetic Study with the Laser-Photolysis / UV Absorption Technique

The apparatus used for these experiments has been described very recently in the literature [4]. It consists of an oven-mounted cell, which is made of 11-mm-i.d. pyrex tubing (80 cm in length) with spectrosil-grade quartz windows. The oven temperature is controlled by a variable resistance and can be raised to about 500 K. The temperature can be controlled to a precision of about 3 K.

Radicals for this study are produced by the photolysis of benzyl bromide using the 248-nm line of a Lamda Physik model EMG 101 excimer laser, whose beam is directed lengthwise through the cell:

(4) $$C_6H_5CH_2Br + h\nu \longrightarrow C_6H_5CH_2 + Br$$

The concentrations of the benzyl radical is monitored by absorption of an UV beam which is produced by a deuterium lamp, collimated by a short focal length lens, and counterpropaged (relative to the laser beam) through the cell. The analysis wavelength for these experiments was 305 nm, where the benzyl radical is known to absorb strongly [14,16]. The 253 nm line is not practical for these experiments due to its proximity to the wavelength of the laser radiation. The UV light from the deuterium lamp is focussed onto the slit of a monochrometer, and the signal is generated by a photomultiplier tube, whose output is followed in real time on a digital oscilloscope. The data are subsequently transferred to a microcomputer for storage, averaging, and analysis.

We found that after several laser shots, soot began to accumulate on the cell quartz windows. This problem was eliminated by introducing a window purge that represented less than 5% of the total gas flow into the cell. The purge gas was preheated

to the experimental temperature and contained the same oxygen concentration as the experimental gas mixture.

The gas mixtures are prepared in an all-teflon-and-glass vacuum line and are passed into the cell via teflon tubing. The gas flows are maintained and measured by calibrated flow controllers. The pressure in the cell is measured by a MKS Baratron pressure gauge. Benzyl bromide is passed into the cell by passing a flow of nitrogen through a bubbler containing the liquid bromide cooled in an ice bath. Typical flows for these experiments are several liters per minute at ambient pressures and several hundred cm^3 per minute at 20 torr. Given the small volume of the cell, we operate the laser at a repetition rates of about 0.1 Hz to ensure that the gas mixture is replenished between each flash. A typical experiment requires about 50 laser shots to obtain a satisfactory signal-to-noise ratio.

The radical precursor benzyl bromide (Aldrich, purity >98%) was degassed before use; oxygen (AGA Gaz spéciaux, purity >99.995%), nitrogen (AGA Gaz spéciaux, purity >99.995%), and synthetic air (same purity and supplier as for N_2 and O_2) were used as supplied.

Results

Kinetic Study by Flash Photolysis

For these and the laser-photolysis experiments described below, values for the rate constant k_1 are derived from the experimental traces by a nonlinear least-squares fitting of the data which uses a set of kinetic differential equations to represent each of the reactions that occur after the flash. For these flash-photolysis experiments, the strong 253-nm absorption feature permitted us to work with low initial benzyl radical concentrations ($4-7 \times 10^{12}$ molecule cm^{-3}); this minimizes secondary reactions that might interfere with the kinetic analysis. The first step for each series of kinetic experiments was the characterization of the benzyl decay in the absence of O_2, both to determine with precision the initial benzyl concentration for the specific set of experimental conditions and to characterize the kinetics in competition with reaction (1) at low O_2 concentrations. After the initial formation of the radicals by flash photolysis, the dominant loss process for the benzyl radical is its self reaction when no oxygen is present. However, in our system, the reaction of benzyl radicals with Cl_2 and with trace concentrations of O_2 in the cell may also contribute to the observed decay:

$$C_6H_5CH_2 + C_6H_5CH_2 \longrightarrow \text{dibenzyl} \quad (5)$$

$$C_6H_5CH_2 + O_2 \xrightarrow{[M]} C_6H_5CH_2O_2 \quad (1)$$

$$C_6H_5CH_2 + Cl_2 \longrightarrow C_6H_5CH_2Cl + Cl \quad (6)$$

The contribution of reaction (6) is assessed from its rate constant [8] and the UV cross-section of benzylchloride at 253 nm [17]. The chlorine atom produced in this reaction reacts with toluene instantaneously (relative to the kinetic timescale) to regenerate a benzyl radical. A rate expression for this process is included in the kinetic optimization routine. Also, trace amounts of oxygen are always present in the cell and can contribute slightly to the observed kinetics for these experiments. The optimized values for k_1 in the absence of O_2 correspond to an impurity on the order

of 5 ppm, and the pseudo-first-order value obtained by these experiments is routinely subtracted from k_1 determined by later experiments (with oxygen) to account for this impurity.

With only small and determinable contributions from the above reactions in the absence of O_2, we attribute the remainder of the benzyl loss to the benzyl radical recombination reaction (5). Although reaction (5) has been previously studied [18], we find that k_5 is about a factor of 10 greater than the value that is calculated by the previously reported Arrhenius parameters. This discrepancy may arise because the earlier study was carried out at elevated temperatures; the extrapolation of the Arrhenius relation into the temperature range valid for this study may not be accurate. Additionally, because the process is second-order with respect to the concentration of the benzyl radical, an overestimate of the cross-section used in our analysis would result in an overcalculation of k_5. The value for the cross-section used in this study is indeed large, 1.0×10^{-16} cm^2 molecule^{-1}; it was evaluated from literature values with a fairly large uncertainty, ca. 50%, due to its dependence on the spectral resolution of the various spectrometers used [14]. With this value, we can in turn calculate that $k_5 = (4.6 \pm 2.5) \times 10^{-11}$ cm^3 molecule^{-1} s^{-1}, corresponding to $k_5/\sigma = (4.6 \pm 0.5) \times 10^5$ cm s^{-1} at 253 nm, with a spectral band width of 2 nm. We found that the rate constant did not vary over the temperature range studied (400–450 K). We remind that the purpose of determining a value of this rate constant was to account for reaction (5) in the overall kinetic scheme for the study of reaction (1); even if the value for k_5 used in the simulations is too large, this is not expected to influence greatly our results on K_p or k_1. As we discuss below, these determinations are sensitive to the ratio k_5/σ (benzyl).

We can then determine k_1 by a series of experiments in which oxygen is added to the cell, keeping the other experimental parameters unchanged. Although only of minor contribution, we include the following two reactions in the full kinetic model:

(7) $$C_6H_5CH_2 + C_6H_5CH_2O_2 \longrightarrow 2C_6H_5CH_2O$$

(8) $$C_6H_5CH_2O_2 + C_6H_5CH_2O_2 \longrightarrow \text{products}$$

The contribution of reaction (8) has been evaluated very recently in a separate set of experiments in this laboratory as a part of a separate research effort [19]. A value of k_7 was estimated from experiments conducted at the higher temperatures of the equilibrium constant determination, described in the next section. Briefly, at temperatures where the redissociation of benzylperoxy into benzyl radicals and O_2 is competitive with association, steady-state concentrations are rapidly established for the benzyl and benzylperoxy radicals; under these conditions, and especially for oxygen concentrations which yield $[\text{benzyl}]_{ss} \simeq [\text{benzylperoxy}]_{ss}$, a kinetic constant for reaction (7) must be introduced into the simulation to account for the loss of total radical concentration of the system. This is carried out by fitting the downward slope of the slowly decaying signal due to the sum of the two absorbing radicals (c.f. Fig. 2). The assumption here is that $C_6H_5CH_2O$, once formed, yields benzaldehyde by subsequent reaction. A sensitivity analysis of the role of reaction (7) in the kinetic scheme showed that it contributes negligibly to the determination of k_1 and K_p. We estimate from this analysis that $k_7 = 5.6 \times 10^{-11}$ cm^3 molecule^{-1} s^{-1} over the entire temperature range of this study. Finally, we note that the reaction between benzyl and benzylperoxy radicals is probably more complicated than the simple mechanism given and that a pressure dependent association channel may exist, but for the purposes of kinetic modelling this potential complication has been neglected.

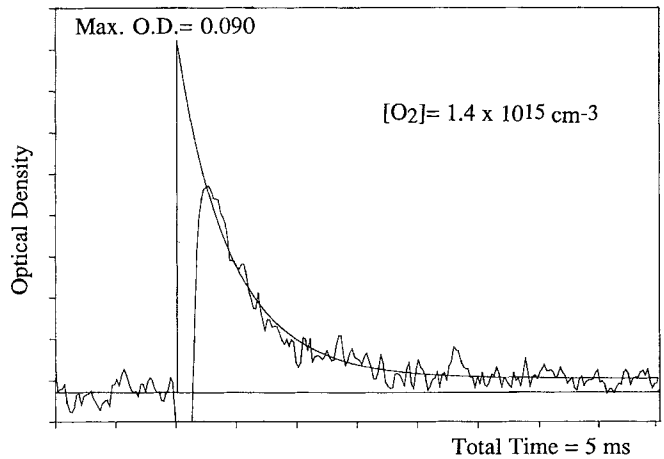

Figure 1. Time-absorption profile of a flash-photolysis experiment conducted at 398 K to determine k_1. The line through the data represents the result of the fitting routine which optimizes k_1 within the kinetic scheme outlined in Table II. The initial absorption was determined in a previous experiment conducted in the absence of O_2 [c.f. Fig. 2(a)]. For this experiment, concentrations in molecule cm^{-3} were: [toluene] = 2.6×10^{15}; [Cl_2] = 4.5×10^{15}; and [O_2] = 1.4×10^{15}.

The contributions of reactions (7) and (8) are small compared with the rapid loss of benzyl radical due to reaction (1) in the presence of O_2. As can be seen in Figure 1, it is important to establish the initial benzyl radical absorption in a control experiment before the addition of oxygen; this establishes unambiguously the starting point of the rapid pseudo-first-order decays of the later experiments. The full set of parameters used in the analysis is given in Table II, and the results are summarized in Table III. The procedure yielded values for the k_1 that are self consistent over a fairly broad range of oxygen concentrations, providing strong evidence that the chemical system is well understood.

TABLE II. Values of kinetic and spectral parameters used in the analysis of the flash photolysis experiments on k_1 and K_p.

Reaction	k(cm^3 $molecule^{-1}$ s^{-1})	Reference
$C_6H_5CH_2 + C_6H_5CH_2 \rightarrow$ dibenzyl	4.5×10^{-11}	This work
$C_6H_5CH_2 + O_2 \rightarrow C_6H_5CH_2O_2$	see text and Table III	This work
$C_6H_5CH_2 + Cl_2 \rightarrow C_6H_5CH_2Cl + Cl$	$5.7 \times 10^{-12} \exp\{-880/RT\}$	[8]
$C_6H_5CH_2 + C_6H_5CH_2O_2 \rightarrow 2C_6H_5CH_2O$	5.6×10^{-11}	This work
$C_6H_5CH_2O_2 \rightarrow C_6H_5CH_2 + O_2$	See text and Table III	This work
$C_6H_5CH_2O_2 + C_6H_5CH_2O_2 \rightarrow$ 2 benzaldehyde	$5.3 \times 10^{-14} \exp\{-1500/RT\}$	[19]

Cross sections for analysis:

Species	$\sigma(253)$[a]	Reference
$C_6H_5CH_2$	1.0×10^{-16}	[14]
$C_6H_5CH_2O_2$	6.6×10^{-18}	[19]
$C_6H_5CH_2Cl$	1.0×10^{-19}	[17]
benzaldehyde	2.8×10^{-19}	[19]

[a] Units are cm^2 $molecule^{-1}$.

TABLE III. Results of flash photolysis and laser-photolysis experiments on k_1.

T (K)	P (torr)	$[O_2]$[a]	k_1 [b]	Technique[c]/ Experiments
298	760	$(2.0\text{-}4.2) \times 10^{16}$	1.43 ± .09	LP/4
323	760	$(0.60\text{-}4.3) \times 10^{16}$	1.38 ± .09	LP/6
323	20	$(0.91\text{-}4.3) \times 10^{16}$	1.36 ± .09	LP/4
323	760	$(7.2\text{-}21.5) \times 10^{14}$	1.36 ± .09	FP/4
363	760	$(0.98\text{-}28.1) \times 10^{16}$	1.32 ± .09	LP/4
363	760	$(6.4\text{-}25.3) \times 10^{14}$	1.18 ± .09	FP/5
398	760	$(5.9\text{-}23.4) \times 10^{14}$	1.25 ± .09	FP/6

[a] Concentration in units of molecule cm^{-3}.

[b] Rate constants are multiplied by 10^{12} and are in units of cm^3 $molecule^{-1}$ s^{-1}.

[c] Techniques are laser photolysis (LP) and flash photolysis (FP).

Equilibrium Constant Determination by Flash Photolysis

The equilibrium constants for reaction (1) were determined by a similar series of experiments, conducted in the temperature range where the residual absorption begins to measurably increase due to the presence of a steady state concentration of benzyl radicals. At these temperatures, the rate of back dissociation, k_{-1}[benzylperoxy], is comparable to the rate of association. The equilibrium constant, which is independent of the oxygen concentration, is determined from the (k_1/k_{-1}) ratio. Equilibrium constants are determined from the experimental traces by fixing the value for $k_1 = 1.2 \times 10^{-12}$ cm^3 $molecule^{-1}$ s^{-1}, a value which is reasonable based on our kinetic measurements at lower temperatures; then the parameter k_{-1} is then optimized for each experiment by fitting the experimental time-absorption profiles to simulated ones using the complete kinetic mechanism (c.f. Table II). Within a series of experiments, the only experimental condition changed is the $[O_2]$. The nature of these experiments is such that the profiles that are observed provide an accurate value for the ratio (k_1/k_{-1}), i.e., the information about the equilibrium is contained in the extent of the absorption immediately following the rapid initial decay. The magnitude of this absorption is determined by the steady-state concentrations of benzyl and benzylperoxy radicals under the specific conditions of temperature and oxygen concentration. Thus, once the total radical concentration is determined, with a given set of cross-sections for the absorbing species the same final value for the ratio (k_1/k_{-1}) will be returned by the optimization routine. Fixing k_1 to an estimated value does not add uncertainty to the resulting value of the equilibrium constant because the fitting routine compensates the value returned for k_{-1} to match the observed absorption. Indeed, this additional uncertainty in k_{-1} is the reason we prefer not to present a kinetic expression for the decomposition of the benzylperoxy radical.

A typical series of experiments to determine the equilibrium constant is shown in Figure 2. As stressed above, the only difference within this series of experiments is the oxygen concentration, varied from zero [(as shown in Figure 2(a)] to a large excess, up to one atmosphere at the highest temperatures studied. In the case of elevated $[O_2]$, the residual signal is due mostly to the benzylperoxy absorption. In the intermediate case of Figure 2(b), the decay of the benzyl radical concentration due to reaction (1) is evident, falling rapidly to the equilibrium concentration ratio of benzyl and benzylperoxy. The conditions used for this series of experiments, along

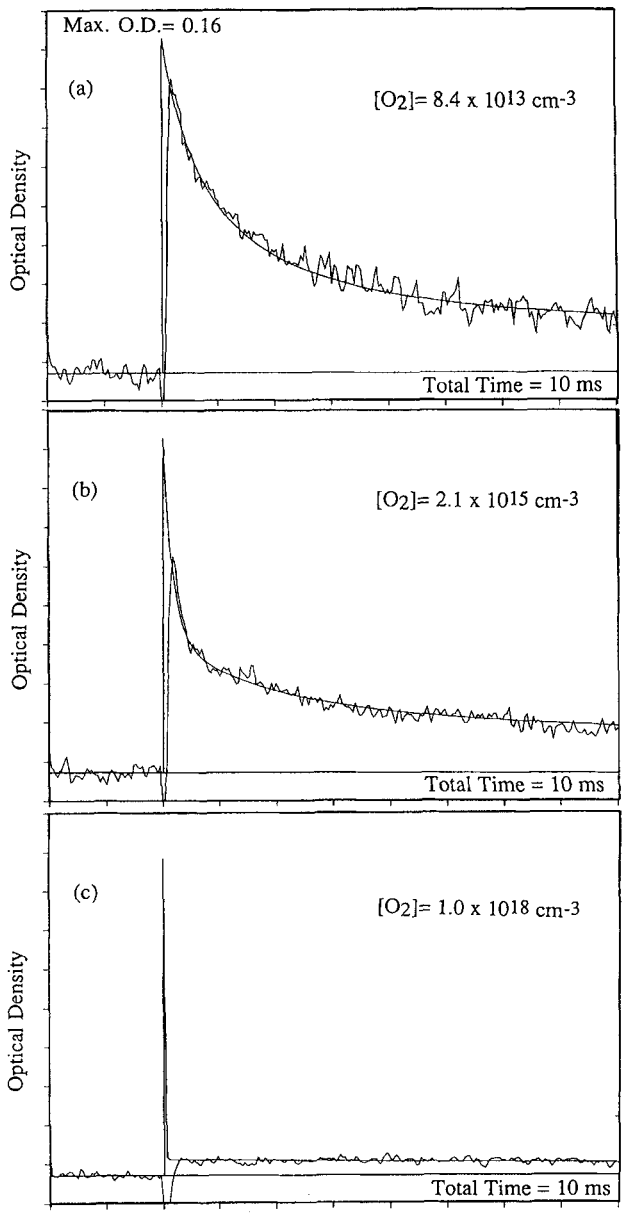

Figure 2. Time-absorption profiles for a series of experiments conducted at 427 K to determine K_p. All experimental parameters are held constant except for $[O_2]$. For this series, concentrations in molecule cm^{-3} were: toluene $= 4.6 \times 10^{15}$ and $[Cl_2] = 6.5 \times 10^{15}$. The $[O_2]$ in (a) corresponds to the 5 ppm background concentration.

with the resulting values of K_c and K_p, are summarized in Table IV. Also in Table IV we give the values of $[O_2]$, k_{-1} and the resulting K_p for a single representative series of experiments conducted at 449 K. The values of $\ln(K_p)$ are plotted as a function of $1/T$ in Figure 3. The expression thus derived from our experiments on K_c is:

$$K_c = (1.75 \pm 0.2) \times 10^{-26} \exp[(10360 \pm 790)K/T] \text{ cm}^3 \text{ molecule}^{-1}$$

TABLE IV. A. Results and conditions of the flash photolysis experiments of K_c and K_p.

T	[tol.][a]	$[Cl_2]$[a]	$[benzyl]_0$[b]	$[O_2]$[c]	K_c[d]	K_p[e]	Exp.
525	3.7	5.4	6.0	4.3-18.9	$(5.2 \pm 2.0) \times 10^{-18}$	$(7.3 \pm 2.8) \times 10^{1}$	7
499	3.9	5.1	6.5	4.6-86.4	$(1.9 \pm 0.7) \times 10^{-17}$	$(2.8 \pm 1.0) \times 10^{2}$	6
487	4.0	6.3	7.0	4.7-88.5	$(3.5 \pm 0.4) \times 10^{-17}$	$(5.3 \pm 0.6) \times 10^{2}$	5
478	4.1	6.0	13.1	2.4-23.6	$(5.9 \pm 2.6) \times 10^{-17}$	$(9.1 \pm 3.9) \times 10^{2}$	5
457	4.3	6.8	9.0	1.0-48.6	$(9.0 \pm 2.3) \times 10^{-17}$	$(1.4 \pm 0.4) \times 10^{3}$	8
449	4.3	7.4	10.2	1.0-25.1	$(1.2 \pm 0.3) \times 10^{-16}$	$(2.0 \pm 0.5) \times 10^{3}$	7
433	2.4	4.1	5.0	0.05-5.44	$(3.7 \pm 1.5) \times 10^{-16}$	$(6.3 \pm 2.5) \times 10^{3}$	7
427	4.6	7.3	12.3	1.1-13.3	$(5.6 \pm 2.1) \times 10^{-16}$	$(9.6 \pm 3.6) \times 10^{3}$	6
420	2.4	4.3	4.7	0.06-1.12	$(9.5 \pm 3.3) \times 10^{-16}$	$(1.7 \pm 0.6) \times 10^{4}$	6
407	4.8	7.0	10.0	1.1-2.8	$(1.5 \pm 0.5) \times 10^{-15}$	$(2.7 \pm 0.9) \times 10^{4}$	4
404	2.5	4.8	4.7	0.06-0.88	$(3.1 \pm 0.6) \times 10^{-15}$	$(5.6 \pm 1.1) \times 10^{4}$	8
398	7.6	4.3	6.3	0.06-0.09	$(3.4 \pm 0.1) \times 10^{-15}$	$(6.3 \pm 0.2) \times 10^{4}$	2

B. Rate constants and K_p as a function of $[O_2]$ for experiments at 449 K.

$[O_2]$[c]	k_{-1}[f]$/10^3$	K_p[e]$/10^3$
1.02	7.9	2.48
2.55	9.1	2.15
5.08	13.2	1.50
7.61	8.7	2.25
10.10	8.4	2.33
12.7	10.2	1.92
25.1	12.8	1.53

[a] Concentrations multiplied by 10^{-15} and in units of molecule cm^{-3}; tol. = toluene.

[b] Concentrations multiplied by 10^{-12} and in units of molecule cm^{-3}.

[c] Concentrations multiplied by 10^{-16} and in units of molecule cm^{-3}.

[d] Equilibrium constants in units of cm^3 $molecule^{-1}$.

[e] Equilibrium constants in units of atm^{-1}.

[f] Rate constants in units of s^{-1}.

Kinetic Study by Laser-Flash Photolysis

For this study, the kinetics experiments were conducted at sufficiently elevated oxygen concentrations to ensure pseudo-first-order decay of the benzyl radical concentration followed by its absorption at 305 nm. Considerations of the secondary chemistry are far less important for this experimental apparatus due to time resolution of the laser technique, which is about a factor of 100 improved relative to the flash-lamp photolysis. The kinetic model that was used in the nonlinear least-squares optimization routine is outlined in Table V. Every series of experiments began with the observation of the benzyl radical decay in the absence of oxygen. Under these conditions, three recombination reactions are possible after the laser flash:

(4) $C_6H_5CH_2Br + h\nu\ (\lambda = 248\ nm) \longrightarrow C_6H_5CH_2 + Br$

(5) $C_6H_5CH_2 + C_6H_5CH_2 \longrightarrow$ dibenzyl

(9) $C_6H_5CH_2 + Br \longrightarrow C_6H_5CH_2Br$

(10) $Br + Br + M \longrightarrow Br_2$

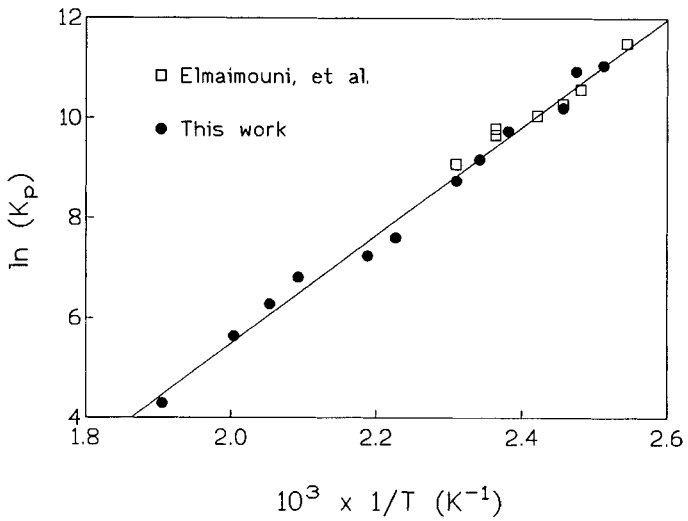

Figure 3. A van't Hoff plot of our experimentally determined equilibrium constants for reaction (1). The straight line represents the Second Law fitting of our data. Of note is the excellent agreement with the only previous determination of $K_p(T)$. The thermochemical parameters derived from the fit are given in the text.

The value for k_5 used in the simulation is that derived in the first part of this study; with this and the previously determined value [20] of k_{10} as kinetic inputs, the optimization routine returns a value for k_9. The value thus determined of $(8.0 \pm 2.0) \times 10^{-11}$ cm^3 molecule^{-1} s^{-1} (for one atmosphere and at 298 K) is in line with values for similar rates of recombination reactions involving alkyl radicals and halogens [20]. A typical time absorption profile for the benzyl radical decay in the absence of O_2 is given in Figure 4(a).

When an elevated concentration of molecular oxygen is present, the decay of the benzyl signal is due almost entirely to the reaction of interest. All the time-absorption profiles are analyzed using the full kinetic model to take into account (1) the small absorption of the peroxyradical product of the reaction, and (2) the small effect of the recombination reactions (5) and (10). It is stressed that, for the elevated oxygen concentrations of this study, a simple pseudo-first-order analysis of the initial

TABLE V. Values of kinetic and spectral parameters used in the analysis of the laser photolysis experiments on k_1.

Reaction	k(cm^3 molecule^{-1} s^{-1})	Refernce
$C_6H_5CH_2 + C_6H_5CH_2 \rightarrow$ dibenzyl	4.0×10^{-11}	This work
$C_6H_5CH_2 + Br \rightarrow C_6H_5CH_2Br$	8.0×10^{-11}	This work
$Br + Br + M \rightarrow Br_2 + M$	$4.08 \times 10^{-34} \times [M] \times \exp\{1.7\ k\text{cal}/RT\}$	[20]
$C_6H_5CH_2 + O_2 + M \rightarrow C_6H_5CH_2O_2 + M$	see text and Table III	This work

Cross sections for analysis:

Species	$\sigma(305)$[a]	Reference
$C_6H_5CH_2$	8.0×10^{-18}	This work
$C_6H_5CH_2O_2$	6.0×10^{-19}	[19]

[a] Units are cm^2 molecule^{-1}.

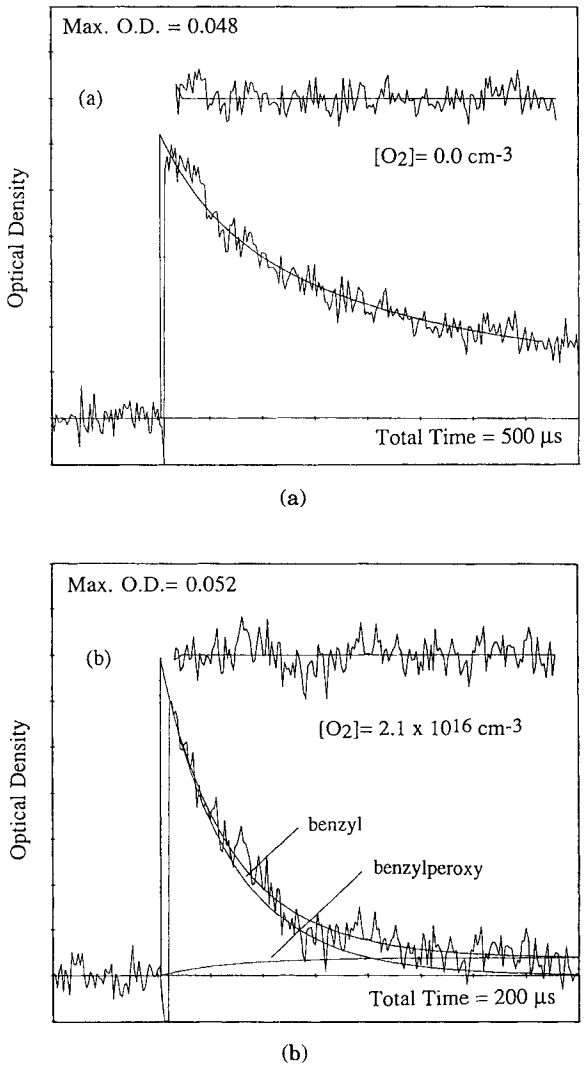

Figure 4. A pair of time-absorption profiles obtained by the laser flash-photolysis apparatus. In (a), the decay of the benzyl radical in the absence of O_2 is shown for an experiment conducted at 298 K and 760 torr of N_2. In (b) a decay of the benzyl radical in the presence of 2.1×10^{16} molecule cm^{-3} of oxygen is shown. The lines through the data represent the optimized fitting of the trace using the kinetic model outlined in Table II. In (b), there are additional curves to show the contributing absorptions of the benzyl and benzylperoxy radicals. The feature at the top of each figure shows the residual to the kinetic fitting.

decay results in a rate constant for reaction (1) that is consistent with the value that returned by the more complex optimization routine within the experimental uncertainty of the determination. A typical benzyl radical decay in the presence of O_2 is shown in Figure 4(b). The results of the experiments as a function of temperature and pressure are given in Table III; in addition, a few representative points for the $k(M,T)$ determination are shown graphically in Figure 5.

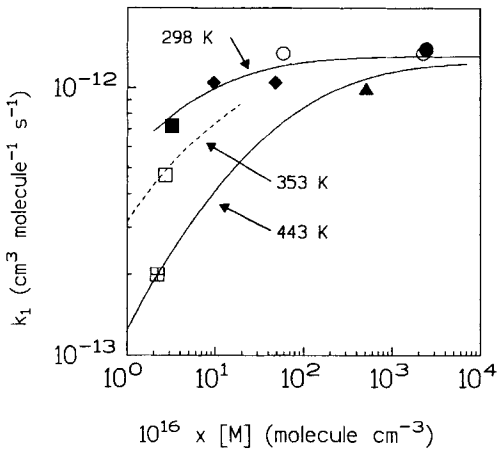

Figure 5. A representation of our and previous results for k_1 presented as a function of temperature and total pressure. Filled symbols represent work conducted at 298 K. Open circles (one partially hidden): laser flash photolysis experiment at 323 K; Closed circle: average of our values at 298 K; Filled triangle: Ebata et al. (in N_2); Filled Diamonds: Nelson and McDonald (in N_2); and Square symbols: Elmaimouni et al. at 298 K, 353 K, and 443 K (in He). The curves show the result of the RRKM fitting routine, carried out for helium bathgas, which is described in the text.

A least-squares fitting of all the kinetic results yield the following expression for k_1 at 760 torr:

$$k_1 = (7.6 \pm 2.4) \times 10^{-13} \exp[(190 \pm 160)K/T)] \text{ cm}^3 \text{ molecule}^{-1} \text{ s}^{-1}$$

Discussion

Thermochemistry of Reaction 1

Values for the enthalpy change of reaction (1) at 298 K, ΔH°_{298}, were obtained by Second- and Third-Law analyses of the equilibrium constant data, using a procedure that has been described previously [3]. In principal, the values of ΔG°_T that are obtained directly from the equilibrium constants must be corrected slightly to account for the variation in ΔH and ΔS between their standard value at 298 K and their value at the temperature where the equilibrium was studied. We found that this effect amounted to less than 1%, so that this correction could be neglected for this determination.

In Figure 3, we show the data graphed in the form of ln K_p vs. $1/T$; by fitting a line through the points, we can calculate the ΔH from the slope and ΔS from the intercept (as $\Delta S/R$):

$$\Delta H^o_{298} = (-89.9 \pm 5.0) \text{ kJ mol}^{-1}$$

$$\Delta S^o_{298} = (-134 \pm 10) \text{ J mol}^{-1} \text{ K}^{-1}$$

The error limits represent the 1σ uncertainties based on the precision of the least-squares fitting to the data. In this Figure 3, we also include the equilibrium constant measurements of Elmaimouni et al. [10] who conducted experiments on K_p over the significantly smaller range of temperatures. It can be seen in this figure that their results are in excellent agreement with our determinations. The difference between

the values they report for ΔH^o_{298} and ΔS^o_{298} using the second-law method arises from the inherent uncertainty of using a narrow range of temperature in a van't Hoff plot.

The other commonly employed procedure for determining the heat of reaction from van't Hoff plots is to rely on a calculation of the ΔS and to use this value either as an additional point in the least-squares fitting of the experimental data or to fix the line to the corresponding value of the intercept and to calculate the slope (ΔH). This procedure can result in a more accurate determination of ΔH when the equilibrium data are taken only over a relatively narrow range of temperature.

The entropy of formation of the benzyl radical at 298 K has been calculated several times previously by using the group method of Benson. A summary of these values are presented in Table VI. More recently, in a study of the thermodynamic properties of the benzyl radical, Hippler and Troe calculated the entropy by using a set of vibrational frequencies derived from spectroscopic studies [18]. They obtained the value of S^0_{298}(benzyl) = 321 J mol^{-1} K^{-1}. In addition, they indicate in a footnote that Tsang, based on a slightly different set of vibrational frequencies, obtained the value of S^0_{298}(benzyl) = 316 J mol^{-1} K^{-1}. Values based on the Benson group method are also available for the benzylperoxy radical, and these are also given in Table VI.

We include in Table VI the values for the entropies calculated from the vibrational frequencies generated using the semi-empirical PM3 method [24]. The frequencies for the vibrational modes thus generated are listed in Table VII, along side a list of experimental values as taken from a recent overview [26] of several determinations of the benzyl radical. In that work, 21 of the 36 fundamental vibrational frequencies have been determined and assigned. There are no experimental results on the vibrational modes of the benzylperoxy radical. It is interesting to organize the experimental assignments alongside those determined by the PM3 calculation, as is done in Table VII, in order to stress the general good agreement between the two, even for the lowest frequency modes which are the most significant for the calculation of a thermochemical parameter. The entropies, S^o_{298}, calculated for the benzyl and benzylperoxy radicals are 316 J mol^{-1} K^{-1} and 346 J mol^{-1} K^{-1}, respectively. From these values, we calculate the ΔS^o_{298} for reaction (1) of (−140 ± 12.5) J mol^{-1} K^{-1}. The error is estimated by taking into account the fact that any over- or under-estimation of vibrational frequencies by the PM3 method is largely cancelled in the determination of a ΔS of reaction.

TABLE VI. Pertinent entropies.

Method, [a] Reference	S^o_{298} (Benzyl) (J mol^{-1} K^{-1})	S^o_{298} (Benzylperoxy) (J mol^{-1} K^{-1})	ΔS^o_{298} [b] (J mol^{-1} K^{-1})
GM, ref. [21]	322.2	401.8	−125.5
GM, ref. [22]	315.1		
GM, ref [23]	342.2	395.5	−133.8
MP, ref. [18]	321.1		
MP, ref. [18][c]	315.6		
MP, this work	316.0	377.7	−140.4

[a] Methods refer to Benson's Group Method (GM) or to a calculation based on the species molecular parameters (MP).

[b] The ΔS^o_{298} is calculated using the following value from ref. [25]: S^o_{298} (O_2) = 204.9 J mol^{-1} K^{-1}.

[c] Work of W. Tsang included in ref. [18] as a footnote.

TABLE VII. Molecular parameters of benzyl and benzylperoxy radicals.

Parameter	Benzyl[a] Calculated	Benzyl Experimental Assignment[b]		Benzylperoxy[a] Calculated
	3172, 3146	C—H str.		2966, 3015
	3097, 3068	C—H str.		3079, 3069
Vibrational	3065, 3055	C—H str.		3059, 3052
Frequencies	3052	C—H str.		3047
(cm^{-1})	1745	C—C ring str.	1554 (8a)	1800
	1724	C—C ring str.	1544 (8b)	1784
	1534	C—C ring str.		1604
	1491	C—C ring str.	1473 (19a)	1544
		O—O str., peroxy		1412
	1382	C—CH2 str.	1266 (7a)	1389
	1306		1306 (3b)	1338
	1249	C—C ring str.	978 ($12a_1$)	1314
	1220	C—H	1164 ($15b_1$)	1225
	1148, 1143	C—H bend 1156, 1076 (9a) (9b)		1153, 1150
	1140	C—H bend	1015 (18a)	1110
	1098, 1037	C—H bend		1098, 1044
	1003	C—H bend		1021
	967	C—H bend	963 ($17a_2$)	986
	961, 924	C—H bend		1246, 1070
		C—O str. peroxy		919
	900	C—C ring def.	817 ($1a_1$)	865
	862	C—H def.	861 (10a)	1002
	834			949
	759	C—H def.	720	850
	624	C—C ring def.	614 (6b)	629
	622		568	777
	544	C—C ring def.	525 (6a)	372
	481		483	584
	443		422 (16b)	672
	396	C—C def.	393 (16a)	351
	324	C—H def.	357 (18b)	533
	172	torsion		467
		additional peroxy		289, 143, 65, 37
Rotational	0.0612			0.0303
Constants[a]	0.0915			0.0348
(cm^{-1})	0.185			0.128
Lennard-Jones Parameters[c]	$\sigma(C_6H_5CH_2O_2) = \sigma(C_6H_5CH_3) = 5.92$ A; σ(He) = 2.608 A			
	$\varepsilon/k(C_6H_5CH_2O_2) = \varepsilon/k(C_6H_5CH_3) = 410$ K; ε/k(He) = 10.22 K			

[a] Calculated with PM3 method, this work.

[b] Assignment guided by work in ref. [26].

[c] Taken from ref. [27].

With this value of the entropy of reaction, we can recalculate the ΔH of reaction by constraining the line of the van't Hoff plot to pass through the intercept which corresponds to our determined value of ΔS°_{298}. The plot is given in Figure 6; from the slope we determine the third law value of $\Delta H^{\circ}_{298} = (-92.5 \pm 4)$ J mol^{-1}. This result is in excellent agreement with our calculated value by the Second-Law method. It is also somewhat larger than the value calculated by Elmaimouni et al., who, in their third-

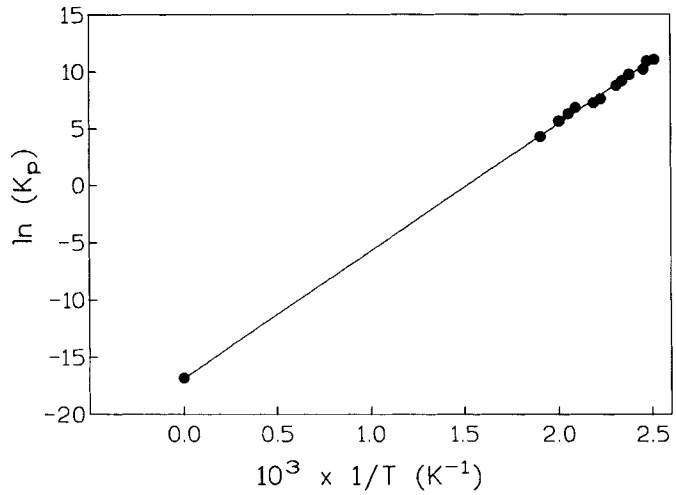

Figure 6. A van't Hoff plot of the equilibrium constants for reaction (1) used to determine a value for ΔH°_{298} using the Third-Law procedure. The value for the intercept was determined from a theoretical determination of ΔS°_{298}, as described in the text.

law analysis, preferred the value of -121 J mol^{-1} K^{-1} for the entropy of reaction, guided by the early work of Benson [21,22] and by their own second-law result.

For this study, we take ΔH°_{298} to be the average of the values obtained by the second-law and third-law analyses: $\Delta H^\circ_{298} = (-91.4 \pm 4)$ kJ mol^{-1}. Once the appropriate ΔC_p is calculated from the structural characteristics given in Table VII, the ΔH°_0 can be determined: $\Delta H^\circ_0 = (-87.9 \pm 4)$ kJ mol^{-1}. This value is used as the critical energy for the RRKM calculation described below.

Enthalpy of Formation of the Benzylperoxy Radical

In the work cited above by Hippler and Troe [18], several equilibria involving the benzyl radical are studied. Based on their experiments, they calculated that $\Delta H^\circ_{f\,298}$ (benzyl) = (210 ± 5) kJ mol^{-1}. In the same article, it is indicated that Tsang calculated that $\Delta H_{f\,298}$(benzyl) = 205 kJ mol^{-1} from the same equilibrium constants using a different value of S°_{298}(benzyl). The difference between the two determinations is not significant, and we take the average to represent the heat of formation: $\Delta H^\circ_{f\,298}$ (benzyl) = (208 ± 4) kJ mol^{-1}. With this value and the heat of reaction quoted above, one can calculate the heat of formation of the benzylperoxy radical: $\Delta H^\circ_{f\,298}$ = (117 ± 6) kJ mol^{-1}.

Analysis of Kinetic Results

In Figure 5, we present representative points of the rate constants for reaction (1) as determined in this work. In sum, we observed no pressure dependence between the pressures of 20 and 760 torr at the temperature of 323 K, and for the experiments conducted at the constant pressure of 760 torr, we see a decrease in k_1 with increasing temperature that is significantly smaller than the experimental uncertainty of the determinations. The agreement between the flash-photolysis and the laser-photolysis experiments is excellent; however, the apparent temperature dependence of k_1 may reflect a small systematic difference between the two techniques. We include in

Figure 5 several points which represent the previous work conducted on reaction (1). At first glance, our results are seen to agree with all the early studies of reaction (1), which concluded that k_1 is independent of both temperature and pressure over the studied range of conditions. The marked pressure dependence observed by Elmaimouni and co-workers, who worked at low pressure using He as the bath gas, poses the possibility of a fall-off effect for reaction (1) under their experimental conditions.

The curves that pass through the data in Figure 5 represent the results of a nonvariational RRKM fitting which explains the ensemble of the experimental observations by invoking a fall-off effect at low pressures of He. This calculation has been carried out using the program "Falloff," which has been described recently in the literature [28]. The program is used to calculate the value of the dissociation rate constants, k_{-1}; these values are then multiplied by the value of the equilibrium constant determined in the previous section to obtain the values for the forward rate of association, k_1. To calculate the rate constants, the structural parameters given in Table VII are adopted. As the Lennard-Jones parameters for the benzyl radical are unknown, we have used the values reported for toluene [27]. The critical energy for the dissociation of benzylperoxy radical, $E°$, is taken to be equal to the enthalpy change for the reaction at 0 K, the assumption being that there is no barrier to this association reaction. The modified Gorin model is adopted to describe the activated complex [29], and the C—O stretch is assumed to be the reaction coordinate. The deformation and torsional modes become two-dimensional restricted rotors at the transition state, a hindrance parameter, η, takes into account the restriction of the rotors. As the calculation was carried out using the modified strong collision hypothesis, the collisional efficiency, β_c, is introduced to account for the fall-off behavior [30].

The RRKM procedure calculates the third-order strong-collision rate constant, k_0^{sc}, using the structural and thermodynamic parameters given in Table VI. The calculation was carried out using He as the bath gas, giving $k_0^{sc} = 5.6 \times 10^{-27} (T/298)^{-6.0}$ cm^6 molecule^{-1} s^{-1}. The parameters β_c and η are adjusted to obtain the best agreement between the calculated and experimental fits. We find that by fixing the value of k_∞ to 1.3×10^{-12} cm^3 molecule^{-1} s^{-1} (independent of temperature), and by using $\beta_c = 0.10 \times (T/298)^{-0.6}$, we are able to reproduce the fall-off effect observed by Elmaimouni et al. at low pressures of helium. This small value for β_c seems reasonable for reaction (1) in helium [31].

The most important conclusion of the RRKM analysis is that, via a calculation of k_0^{sc}, the experimental determination of the equilibrium constant as a function of temperature is shown to be coherent with the various kinetic studies carried out over conditions varied in terms of bath gas, temperature, and pressure. To cast our results in terms of a commonly used version of the Troe expression [30], for which the value of F_c is always taken to be 0.6 [32], we find that the following expressions for k_0 and k_∞ describe reasonably well the ensemble of kinetic results (for He bath gas). We note that since the kinetic experiments were conducted far from the low pressure limit, the quoted value for k_0, whose quoted error represents the 1σ statistical limits of the curve fitting routine, must be considered highly uncertain. The expressions allow one to recalculate the experimental data shown in Figure 5 to within 20% using the functions provided in ref. [32]:

$$k_0 = (1.9 \pm 0.1) \times 10^{-28} (T/300)^{(-6.8 \pm 0.5)} \text{ cm}^6 \text{ molecule}^{-2} \text{ s}^{-1}$$

$$k_\infty = (1.4 \pm 0.1) \times 10^{-12} (T/300)^{(-0.2 \pm 0.2)} \text{ cm}^3 \text{ molecule}^{-1} \text{ s}^{-1}$$

Summary and Conclusion

We report measurements of the equilibrium constant that were carried out over a significantly larger range of temperature than the only previous determination. The good agreement between our results derived from Second-Law and Third-Law methods provides evidence that the temperature range is sufficiently large to obtain reasonably accurate thermodynamic properties. In addition, the results are in excellent agreement with those of the only previous determination of the equilibrium constant. The information that we derived from this study, in particular the heat of formation of the benzylperoxy radical, may prove useful for the thermodynamic assessment of benzylperoxy radical reactions with other species under conditions relevant to atmospheric chemistry and combustion. We report the results of experiments to determine k_1 under varied conditions of pressure and temperature which, at first glance, appear to collaborate the first two studies of reaction (1), where no dependence on the pressure or temperature were observed. Finally, we report the results of a calculation that not only manages to connect theoretically the measurements of the forward rate constant, k_1, with the equilibrium constant K_p, but, in this case, it also unifies several kinetic studies by explaining the origin of an apparent discrepancy between sets of experimental data as a fall-off effect. The utility of the nonvariational RRKM theory as a fitting method is well illustrated by this study of the kinetics and equilibrium of reaction (1).

Acknowledgment

We thank Marie-Therèse Rayez for her PM3 calculations on the benzyl and benzylperoxy radicals. Funding was provided by the CEC (LACTOZ Programme).

Bibliography

[1] R. A. Cox in *Modern Gas Kinetics,* M. J. Pilling and I. W. M. Smith, Eds., Blackwell Scientific, Oxford, 1987; sections 2 and 3.
[2] R. Atkinson, *Atmos. Environ.,* **24A,** 1 (1990).
[3] J. J. Russell, J. A. Seetula, D. Gutman, F. Danis, F. Caralp, P. D. Lightfoot, R. Lesclaux, C. F. Melius, and S. M. Senkan, *J. Phys. Chem.,* **94,** 3277 (1990).
[4] F. F. Fenter, P. D. Lightfoot, J. K. Niirannen, and D. Gutman, *J. Phys. Chem.,* **97,** 5313 (1993).
[5] F. F. Fenter, P. D. Lightfoot, F. Caralp, R. Lesclaux, J. T. Niiranen, and D. Gutman *J. Phys. Chem.,* **97,** 4695 (1993).
[6] B. J. Finlayson-Pitts and J. N. Pitts, Jr., *Atmospheric Chemistry: Fundamentals and Experimental Techniques,* Wiley, New York, 1986.
[7] T. Ebata, K. Obi, and I. Tanaka, *Chem. Phys. Lett.,* **77,** 480 (1981).
[8] H. H. Nelson and J. R. McDonald, *J. Phys. Chem.,* **86,** 1242 (1982).
[9] M. Bartels, J. Edelbutter-Einhauss, and K. Hoyermann, *22nd Symp. (Int.) Combust.,* 1041 (1988).
[10] L. Elmaimouni, R. Minetti, J. P. Sawerysyn, and P. Devolder, *Int. J. Chem. Kinet.,* **25,** 399 (1993), and references therein on previous work in the same laboratory on reaction (1).
[11] P. D. Lightfoot, R. Lesclaux, and B. Veyret, *J. Phys. Chem.,* **94,** 700 (1990).
[12] F. P. Tully, A. R. Ravishankara, R. L. Thompson, J. M. Nicovich, R. C. Shah, N. M. Kreutter, and P. H. Wine, *J. Phys. Chem.,* **85,** 2262 (1981).
[13] T. J. Wallington, L. M. Skewes, and W. O. Siegl, *J. Photochem. Photobiol. A: Chem.,* **45,** 167 (1988).
[14] N. Ikeda, N. Nakashima, and K. Yoshihara, *J. Phys. Chem.,* **88,** 5803 (1984), and the references they cite.

[15] D. Maric, J. P. Burrows, R. Meller, and G. K. Moortgat, *J. Protochem. Photobiol. A: Chem.*, **70,** 205 (1993), and references cited therein.
[16] H. Hiratsuka, T. Okamurra, I. Tanaka, and Y. Tanizaki, *J. Phys. Chem.*, **84,** 285 (1980).
[17] D. Lang, *Absorption Spectra in the Ultraviolet and Visible Region,* L. Lang, Ed., Publishing House of the Hungarian Academy of Sciences, Budapest, 1961.
[18] H. Hippler and J. Troe, *J. Phys. Chem.*, **94,** 3803 (1990).
[19] B. Nozière, D. M. Rowley, R. Lexclaux, M. D. Hurley, and T. J. Wallington, private communication concerning the benzylperoxy radical UV spectrum, and benzylperoxy self reaction rate constant, and the benzylperoxy + HO_2 reaction rate constant. The manuscript is in preparation.
[20] F. Westley, J. T. Herron, R. F. Hampson, and W. G. Mallard, *NIST Chemical Kinetics Database,* NIST Standard Ref. Database 17 US Dept. of Commerce, 1992.
[21] S. W. Benson, *J. Am. Chem. Soc.*, **87,** 972 (1965).
[22] S. W. Benson, *Thermochemical Kinetics,* Wiley, New York, 1976.
[23] E. Ritter and J. Bozzelli, *Thermodynamic Property Estimations of Gas-Phase Radicals and Molecules,* 23rd Symposium (Int.) on Combustion, Orleans, France, 1990.
[24] J. J. P. Stewart, *J. Computational Chem.*, **10,** 209 (1989).
[25] D. R. Stull and H. Prophet, *JANAF Thermochemical Tables,* 2nd ed., National Bureau of Standards, NSRDS-NBS 37, 1971.
[26] F. W. Langkilde, K. Bajdor, and R. Wilbrandt, *Chem. Phys. Lett.*, **193,** 169 (1992).
[27] F. M. Mourtis and F. H. A. Rummens, *Can. J. Chem.*, **55,** 3007 (1977).
[28] W. Forst, *QCPM,* **13,** 119 (1993).
[29] J. W. Davies and M. J. Pilling, *Bimolecular Collisions: Advances in Gas Phase Photochemistry and Kinetics,* M. N. R. Ashfold and J. E. Baggott, Eds., Royal Society of Chemistry, 1989.
[30] W. C. Gardiner, Jr., Ed., *Combustion Chemistry,* Springer-Verlag, New York, 1984.
[31] T. C. Tardy and R. J. Malins, *J. Phys. Chem.*, **83,** 93 (1979).
[32] W. B. DeMore, S. P. Sander, D. M. Golden, M. J. Molina, R. F. Hampson, M. J. Kurylo, C. J. Howard, C. E. Kolb, and A. R. Ravishankara, *Chemical Kinetics and Photochemical Data for Use in Stratospheric Modeling,* JPL Publication 92-20, 1992.

Received May 17, 1993
Accepted July 6, 1993